Advances in Nano Research, *Vol. 15, No. 4 (2023) 355-366*
https://doi.org/10.12989/anr.2023.15.4.355

Green synthesis of silver nanoparticles to the microbiological corrosion deterrence of oil and gas pipelines buried in the soil

Zhi Zhang[1], Jingguo Du*[2] and Tayebeh Mahmoudi[3]

[1]*Shaanxi Geological Construction Land Survey, Planning and Design Institute Co., Ltd, Xi'an 710082, Shaanxi, China*
[2]*Collaborative Innovation Center of Green Development and Ecological Restoration of Mineral Resources, North China University of Science and Technology, Tangshan 063210, Hebei, China*
[3]*Hoonam Sanat Farnak, Engineering and Technology knowledge-based enterprise Company, Iran*

(*Received December 14, 2022, Revised July 1, 2023, Accepted July 24, 2023*)

Abstract. Biological corrosion, a crucial aspect of metal degradation, has received limited attention despite its significance. It involves the deterioration of metals due to corrosion processes influenced by living organisms, including bacteria. Soil represents a substantial threat to pipeline corrosion as it contains chemical and microbial factors that cause severe damage to water, oil, and gas transmission projects. To combat fouling and corrosion, corrosion inhibitors are commonly used; however, their production often involves expensive and hazardous chemicals. Consequently, researchers are exploring natural and eco-friendly alternatives, specifically nano-sized products, as potent corrosion inhibitors. This study aims to environmentally synthesize silver nanoparticles using an extract from Lagoecia cuminoides L and evaluate their effectiveness in preventing biological corrosion of buried pipes in soil. The optimal experimental conditions were determined as follows: a volume of 4 ml for the extract, a volume of 4 ml for silver nitrate (AgNO3), pH 9, a duration of 60 minutes, and a temperature of 60 degrees Celsius. Analysis using transmission electron microscopy confirmed the formation of nanoparticles with an average size of approximately 28 nm, while X-ray diffraction patterns exhibited suitable peak intensities. By employing the Scherer equation, the average particle size was estimated to be around 30 nm. Furthermore, antibacterial studies revealed the potent antibacterial activity of the synthesized silver nanoparticles against both aerobic and anaerobic bacteria. This property effectively mitigates the biological corrosion caused by bacteria in steel pipes buried in soil.

Keywords: green synthesis; microbiological corrosion; silver nanoparticles; soil; steel pipe

1. Introduction

Nanotechnology is the science of manipulating materials at the atomic or molecular scale. It involves the precise control and arrangement of atoms and molecules to create complex structures with unique atomic properties. Considered as the fourth wave of industrial revolution, nanotechnology has rapidly permeated various scientific disciplines and represents one of the fastest-growing fields of technology (Soltani *et al*. 2022). Materials at the nanoscale exhibit distinct physical properties compared to their bulk counterparts. This can be attributed to the increased freedom of motion that atoms and molecules possess at the nanoscale, which directly influences their chemical and physical characteristics (Zhu and Wu 2023). Among the various products of nanomaterials, nanoparticles play a significant role.

Nanoparticles are particles with diameters ranging from 1 to 100 nanometers (Alsultan Abdulmajeed 2021, Dai *et al*. 2021, Alimoradlu and Zamani 2022, Behdinan and Moradi-Dastjerdi 2022, Thakur *et al*. 2022, Zhao *et al*. 2022). Due to their size, they are not visible under conventional light microscopes, necessitating the use of electron microscopes or laser microscopes for observation (Baalousha 2009). The increasing ratio of surface area to volume as particle size decreases leads to a dominance of surface atoms' behavior over those in the bulk material. Consequently, this phenomenon impacts the particle's isolation properties and interactions with other substances (Dingreville *et al*. 2005). Given the expanding application of nanotechnology across various industries, there is a growing demand for diverse types of nanoparticles. Nanoparticles can be produced using two general approaches: top-down and bottom-up methods. In top-down methods, mechanical tools are employed to reduce bulk particles to the nanoscale (Cheng *et al*. 2023, Guo *et al*. 2023, Huang *et al*. 2023, Tang *et al*. 2023, Wu *et al*. 2023, Zhao *et al*. 2023).

Green chemistry is a research methodology that encompasses the design, development, and efficient production of products with minimal health hazards by reducing the use of hazardous substances. The emerging field of green technology aims to mitigate the potential risks associated with nano applications for both humans and the environment (Ding and She 2021, Cuong Bui 2022, Soltanieh *et al*. 2022, Wu *et al*. 2022). The chemical synthesis of nanoparticles, commonly employed today, has raised significant concerns due to the use of hazardous and toxic chemicals, as well as their environmental impact. Nanoparticles possess unique characteristics, including size, shape, and morphology, that profoundly influence various aspects of human life. Consequently, they find diverse applications across scientific disciplines such as medicine, engineering, and healthcare (Tang *et al*. 2005).

*Corresponding author, Ph.D.,
E-mail: jingguodu@126.com

ISSN: 2287-237X (Print), 2287-2388 (Online)

Silver nanoparticles (AgNPs) are crucial and extensively utilized particles in the field of nanotechnology (Ebrahimi *et al*. 2017, Ghadiri *et al*. 2017c, Shahabinejad *et al*. 2018, Shafiei *et al*. 2020). Their remarkable physical and chemical properties make them particularly suitable for electronic components. Moreover, AgNPs have diverse applications in optics, medicine, hygiene, and catalysis. Consequently, the synthesis of these nanoparticles is of utmost importance. Research indicates that AgNPs synthesized using green methods possess antimicrobial, antioxidant, and anti-inflammatory effects. The antimicrobial properties of silver have been recognized for a long time, leading to its widespread use in various applications (Beyene *et al*. 2017). Recent advancements in technology and AgNP production have significantly enhanced their antibacterial activity (Fu *et al*. 2020, He *et al*. 2023, Kashif *et al*. 2023, Li *et al*. 2023). The increased surface-to-volume ratio of silver nanoparticles enhances their antimicrobial and antibacterial efficacy. The integration of nanosilver into antibacterial agents holds promise for combating bacteria (Tang and Zheng 2018).

Silver nanoparticles have the ability to interfere with the functioning of bacterial cells (Ehyaei *et al*. 2017, Ghadiri *et al*. 2017a, b, Shivanian *et al*. 2017). As the size of the silver atom cluster decreases, the surface-to-volume ratio increases, leading to enhanced antibacterial properties. This increase in antibacterial efficacy is particularly notable when the dimensions of the silver particles approach the nano scale, resulting in the formation of nanosilver. The antibacterial properties of silver nanoparticles make them valuable in numerous industries (Vijayakumar *et al*. 2013).

Corrosion is a natural process that occurs when materials reach their lowest free energy level, resulting in their destruction through reactions with the surrounding environment (Azimi *et al*. 2016, Ghadiri *et al*. 2016a, b, Shafiei *et al*. 2016, 2017). The main cause of corrosion in metals is chemical reactions, particularly oxidation. Rust and patina are common corrosion products that form on the metal surface. Removing these deposits exposes the metal to further corrosion (Uhlig and Revie 1985). Corrosion typically involves three main components: metal, oxygen, and an electrolyte. Oxidation and reduction reactions drive the corrosion process. The corroded metal acts as an anode, releasing ions and electrons during oxidation (Tian *et al*. 2022). Oxygen, in turn, is reduced by accepting electrons, leading to the formation of hydroxide ions and cathodic reactions. As the metal in the anode corrodes, metal ions in the hydrated solution form solid compounds on the metal surface. In some cases, oxidation continues and corrosion progresses, while in others, the formation of a protective layer on the corroded surface halts the process (Zehra *et al*. 2022). Nearly all environments have some level of corrosiveness, with variations in severity. Microorganisms are ubiquitous in nature and thrive in air, soil, and water. Microbes that engage in biofouling, biodegradation, and biocorrosion processes are particularly abundant, as they exhibit remarkable tolerance to extreme environmental conditions such as pH, temperature, pressure, and metal concentrations. Corrosion is defined as the destruction or deterioration of metals and alloys through chemical or electrochemical means (Zhang *et al*. 2021, 2023, Yang *et al*. 2023, Yuan *et al*. 2023). Microorganisms' involvement in metal corrosion can be categorized as biological corrosion and microbial corrosion (MIC), which refer to electrochemical processes facilitated or accelerated by microorganisms (Wang *et al*. 2022a). Both uniform and microbial corrosion are driven by electrochemical reactions, with microbes often acting as catalysts. MIC can occur under various conditions, including aerobic, anaerobic, acidic, neutral, or alkaline environments. It encompasses multiple corrosion mechanisms and cannot be universally classified into distinct types. MIC can manifest as localized attacks such as pitting, crevice corrosion, dealloying, and corrosion by precipitation. It can also accelerate galvanic corrosion, stress corrosion, and hydrogen cracking (Kalajahi *et al*. 2022). MIC occurs in various environments, particularly terrestrial, freshwater, and marine settings. Microbial accumulation and the formation of biofilms, consisting of biological substrates and metabolic products, play a crucial role in MIC and require further elucidation (Shokri and Sanavi Fard 2022). Initially, fine sediments, due to bacterial adhesion, form, followed by the attachment of fungi, algae, sea urchins, oysters, and other organisms, leading to the formation of coarse sediments. Sulfate-reducing bacteria (SRB) are among the bacterial groups that play a significant role in the corrosion of steel, such as pipelines (Yang *et al*. 2022). These bacteria produce corrosive substances such as mineral or organic acids, ammonia, sulfides, and phosphoric compounds, which can degrade passive and protective layers on metals and alloys like aluminum, stainless steel, chrome, and nickel (Iverson 1987).

These organisms oxidize iron ions to ferric ions, resulting in the deposition of iron hydroxides within the biofilm (Omidi *et al*. 2013, Ghadiri *et al*. 2016c, Mousavi *et al*. 2017). Anaerobic bacteria, such as sulfate-reducing bacteria (SRB), are capable of colonizing the crevices formed in mild steel pipelines (Wang *et al*. 2022b). Aerobic bacteria can contribute to corrosion through various mechanisms, including sludge formation, oxidation of iron and sulfides, and production of acidic metabolites. The accumulation of hydrated bacterial sludge on metal surfaces creates localized differences and provides an environment for the growth of subsequent anaerobic organisms. Soil, as a corrosive environment, exhibits a high degree of complexity compared to other environments. The corrosion rate in soil can vary widely, ranging from rapid to minimal corrosion (Boulmedais *et al*. 2004). This complexity is evident from the fact that some pipes corrode within a year, while ancient iron objects buried in the ground have remained relatively free from severe corrosion for hundreds of years (Kuang *et al*. 2007) (Fig. 1).

Lagoecia cuminoides L., commonly known as wild cumin, belongs to the Apiaceae family. It is an herbaceous perennial plant with a thick stem measuring 2-3 cm in diameter and reaching up to 2 meters in length. The leaves of this plant are thick, with several dark green and glossy leaflets. Its flowers are small and yellow, arranged in compound umbels. The fruit is a yellow-brown egg-shaped structure measuring less than one centimeter in length. Wild cumin grows in various parts of Asia. Research on this plant

Fig. 1 Biological corrosion of pipes buried in the soil

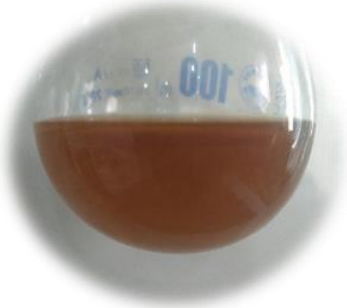

Fig. 2 Silver nanoparticles

has demonstrated its antioxidant properties and antimicrobial activity. The main phenolic compounds found in L. cuminoides are chlorogenic acid, hesperidin, rosmarinic acid, and vanillin (Bahmanzadegan *et al*. 2019b). Considering the side effects and disadvantages associated with chemical preservative compounds, medicinal plants and natural compounds can be used as alternatives for synthesizing nanoparticles, aiming to achieve certain properties, such as antimicrobial effects. In green synthesis, plants and microorganisms serve as reducing agents for the production of metal nanoparticles and metal oxides (Liu *et al*. 2021, Wang *et al*. 2022c, Nie *et al*. 2023, Ran *et al*. 2023). The choice of reducing agent significantly influences the morphology, size, and physical and chemical properties of the particles (Farnsworth and Soejarto 1991). Plant sources that contain carboxylic, amine, protein, and carbohydrate groups in their extracts play a crucial role in the absorption and biological regeneration process required for nanoparticle formation. Additionally, factors such as time, temperature, light, and other parameters can also influence the size and shape of the nanoparticles (Bahmanzadegan *et al*. 2019a).

According to previous investigations, no research has been conducted on the synthesis of silver nanoparticles using Lagoecia cuminoides L. to prevent biological corrosion. Therefore, the aim of this study is to employ a green synthesis method to produce silver nanoparticles by extracting Lagoecia cuminoides L. Furthermore, the antibacterial properties of these synthesized nanoparticles will be investigated in order to prevent the biological corrosion of steel pipes buried in the soil. Microbial accumulation on the surface of these pipes leads to rust formation and subsequent corrosion.

2. Materials

The list of materials and devices employed for the green synthesis of silver nanoparticles, utilizing environmentally friendly plant extracts to combat bacterial agents responsible for biological corrosion in soil, is as follows: $AgNO_3$ (purity: 99.9%), hydrochloric acid (HCl, purity: 37%), and sodium hydroxide (NaOH, purity: 96%). All materials utilized in this study were procured from Merck.

Additionally, several analytical techniques were employed to comprehensively investigate the synthesized nanoparticles. These techniques include ultraviolet/visible spectroscopy (UV-Vis), transmission electron microscopy (TEM), and infrared spectroscopy (IR). These instruments were utilized to characterize the synthesized nanoparticles and gather further insights into their properties.

3. Methods

3.1 Lagoecia cuminoides L extraction

After cleaning and washing, the plant was dried in the shade and ground to conduct the test. Twenty grams of the dried powder were transferred to a beaker containing 200 ml of distilled water. The mixture was stirred using a stirrer for one hour while simultaneously applying ultrasonic waves (30 kHz, 40 minutes). Subsequently, the mixture was centrifuged at a rate of 4000 rpm for 10 minutes. To the obtained extract, 10-15 ml of methanol was added, and it was left at a temperature of 15 °C for 24 hours until a fat-free extract was obtained. For dehydration, the defatted extract was dissolved in dichloromethane and dried using magnesium sulfate. The resulting mixture was desolvated in a rotary evaporator under vacuum until a pure extract was obtained. To concentrate the methanolic extract, it was placed in a water bath at a temperature of 70°C.

3.2 Green synthesis of Silver nanoparticles

To prepare silver nanoparticles with a uniform shape and size, the study investigated the effects of various parameters. This included analyzing the impact of pH, extract concentration, and $AgNO_3$ concentration, as well as the influence of time and temperature on nanoparticle synthesis.

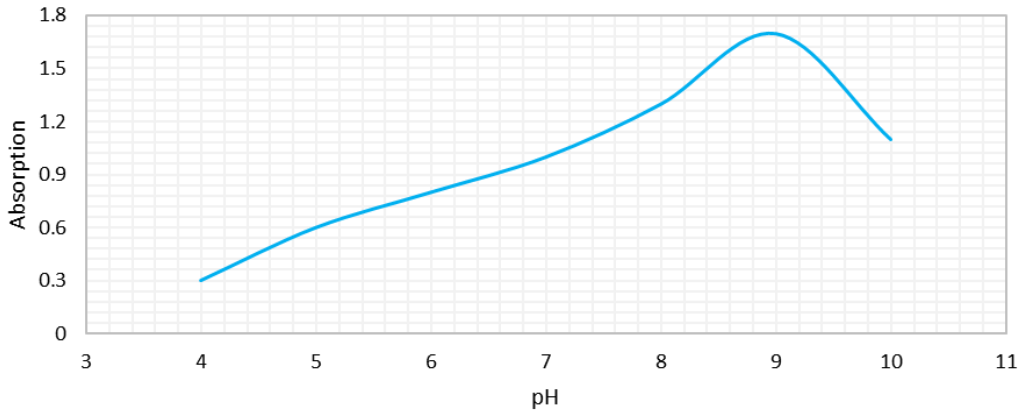

Fig. 3 Absorption changes related to silver nanoparticles at different pH

To initiate the process, 3 ml of the sample extract was added to 3 ml of a 3 mM $AgNO_3$ solution. The pH of the mixture was adjusted to 9 using 1 M NaOH and hydrochloric acid. Subsequently, the solution was maintained at a temperature of 70 °C for 30 minutes. A color change from pale yellow to dark brown indicated the formation of silver nanoparticles (Fig. 2). The extract containing the nanoparticles was then subjected to centrifugation at 4000 rpm for 15 minutes. The resulting sediment was dried in an oven at 70 °C for 3 hours.

3.3 Ultraviolet/visible spectroscopy (UV-Vis)

In order to determine the maximum wavelength of absorption, 250 microliters of the solution containing the extract and silver nitrate were diluted to a volume of 1 ml with distilled water. The solution was then subjected to spectrometry analysis, specifically checking for ultraviolet/ visible wavelengths within the range of 300-700 nm. The solution containing silver nanoparticles exhibited maximum absorption at approximately 430 nm. The presence of a peak in this specific region confirms the successful synthesis of silver nanoparticles, as the peak at wavelengths between 400 and 450 nm is attributed to the Surface Plasmon resonance of the nanoparticles, resulting from the induction of free electrons. In this study, the identification of biomolecules in the plant extracts that can convert silver nitrate into silver nanoparticles was carried out using infrared spectroscopy (IR). Furthermore, the size and morphology of the synthesized silver nanoparticles were examined through transmission electron microscope (TEM) imaging. To investigate the properties of the silver nanoparticles, X-ray diffraction (XRD) analysis was employed.

4. Investigating the antibacterial effects of synthesized nanoparticles disc release method

Standard bacterial strains of Staphylococcus aureus and Desulfococcus were cultured on Mueller Hinton agar at 37 degrees Celsius. Subsequently, various concentrations of silver nanoparticles synthesized in deionized water (100, 60, 30 µg/µl) were applied to sterilized plates with a diameter of 6 mm using an autoclave. Following incubation at 37 °C for 24 hours, the diameter of the inhibition zone devoid of bacterial growth was measured and recorded in millimeters.

4.1 Investigating Minimum inhibitory concentration (MIC) by the method of microdilution

In this method, different concentrations of silver nanoparticles were tested against bacteria using a 96-well microplate. Initially, 95 microliters of Muller Hinton medium were dispensed into each of the 96 wells. Next, 100 µl of silver nanoparticles at a concentration of 100 µg/µl were added to the first well. The contents of the first well were thoroughly mixed, resulting in a half-dilution of the nanoparticles. Subsequently, 100 µl was transferred from the first well to the second well, and this process was repeated to create a dilution series until reaching the last well. The last well served as a negative control, containing 195 microliters of Muller Hinton solution and 5 microliters of microbial suspension without the tested compound. The total volume of each well was 200 microliters. Subsequently, all the wells except well number 12 were inoculated with 5.5 µl of bacterial suspension, equivalent to 1.6 × 108 CFU/ml. The microplates were then incubated at 37 °C for 24 hours with the lid closed. After incubation, the turbidity of the wells was visually assessed to observe bacterial growth or absence thereof.

4.2 Determining the minimum bactericidal concentration of nanoparticles (MBC)

The wells without turbidity, indicating bacterial growth inhibition, were selected, and the bacteria from these wells were cultured on Mueller Hinton agar medium using a sterile loop. The agar plates were then incubated at 37 degrees Celsius for 24 hours. The minimum concentration of nanoparticles at which no bacterial survival was observed is defined as the Minimum Bactericidal Concentration (MBC). In this study, the effect of the synthesized nanoparticle on the standard sample was replicated three times, and two control groups were included for each dilution series.

Table 1 Optimizing pH, Extract volume (ml), $AgNO_3$ volume (ml), Time, and Temperature to prepare silver nanoparticles

Solution number	pH	Extract volume (ml)	$AgNO_3$ volume (ml)	Time	Temperature
1	4	1	1	20	20
2	5	2	2	40	30
3	6	3	3	60	40
4	7	4	4	80	50
5	8	5	5	100	60
6	9	-	-	-	70
7	10	-	-	-	80
8	-	-	-	-	90
9	-	-	-		100
The results	9	4 ml	4 ml	60 min	60°C

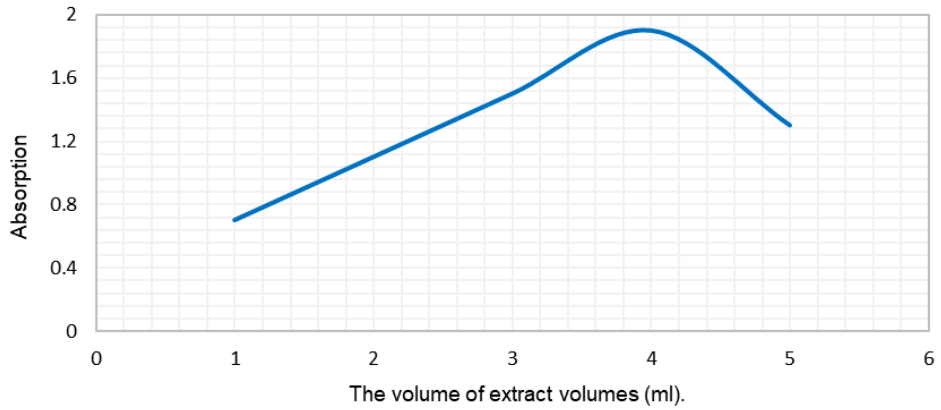

Fig. 4 Absorption changes related to silver nanoparticles at different extract volumes.

5. Results

5.1 pH optimization

To optimize the pH value, a solution containing 2 milliliters of extract and 5 milliliters of silver nitrate (3mM) was prepared. Two solutions, NaOH and HCl with a concentration of 1 M, were used to adjust the pH of the solutions. Seven solutions with different pH values were prepared and their details are shown in Table 1. The absorbance of each solution was measured at a wavelength of 430 nm. As depicted in Fig. 3, the solution at pH = 9 exhibited the highest absorption rate. This suggests that silver nanoparticles are most stable and have a relatively smaller size at pH = 9. Therefore, pH = 9 was selected as the optimum condition based on the absorbance measured by the spectrophotometer.

5.2 Optimizing the extract volume

Five batches of solutions were prepared to optimize the extract concentration. Each group of solutions had different concentrations of the extract, while the concentration of silver nitrate salt (3 mM) remained constant across all five groups, as shown in Table 1. The volume of silver nitrate solution used was 5 ml, and the final volume of the extract and silver nitrate mixture was set at 10 ml for all experiments. After 40 minutes, each batch of solutions changed color to brown. The absorption spectrum of each solution was immediately recorded at a wavelength of 430 nm using a visible-ultraviolet spectrophotometer. The resulting diagram is presented in Fig. 4. Based on the absorption spectrum, it can be observed that the optimal volume of the plant extract is 4 ml, as it exhibited a higher absorption spectrum.

5.3 Optimizing the volume of $AgNO_3$

First, a 3 mM solution of silver nitrate salt was prepared, and then different volumes of this solution were added to the reaction as indicated in Table 1. The absorption spectrum of the resulting solutions was recorded at a wavelength of 430 nm using a spectrophotometer, and the results are shown in Fig. 5. It was observed that the absorption volume of the solution did not exhibit significant changes after reaching a volume of 4 ml of silver nitrate salt with a concentration of 3 mM. Therefore, 4 ml was determined as the optimized volume for the experiment.

5.4 Optimizing reaction time

It was observed that a color change occurred as soon as the reactants were mixed. To optimize the reaction, the absorption of the solution was measured at several time

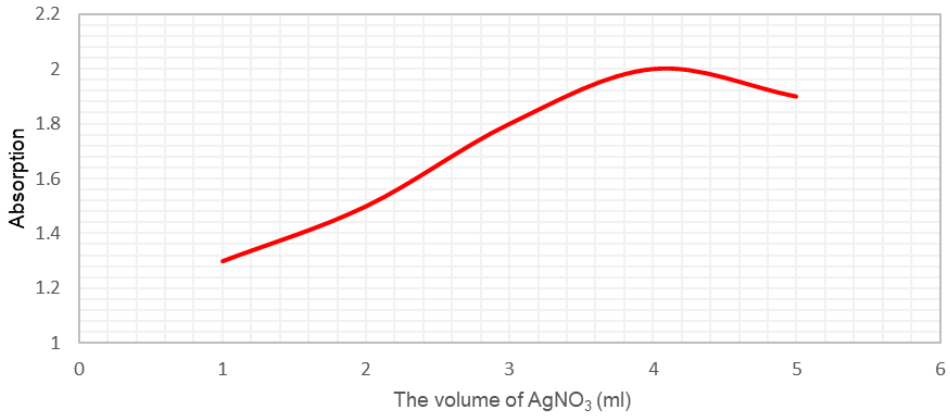

Fig. 5 Absorption changes related to silver nanoparticles at different extract volumes (3mM)

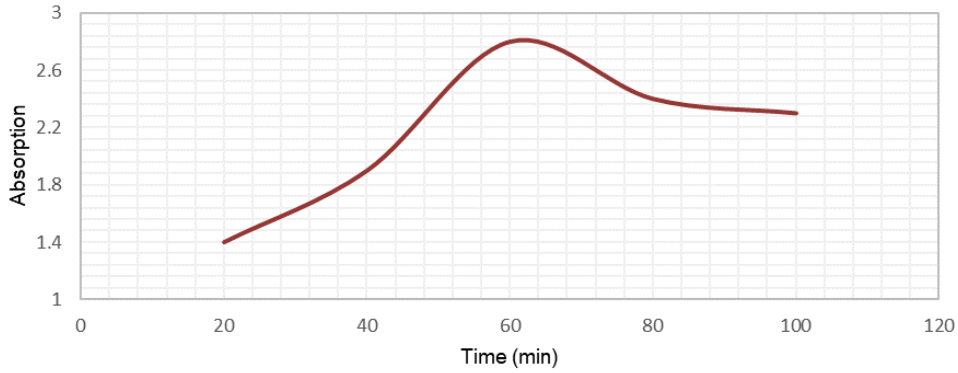

Fig. 6 Absorption changes related to silver nanoparticles at different times

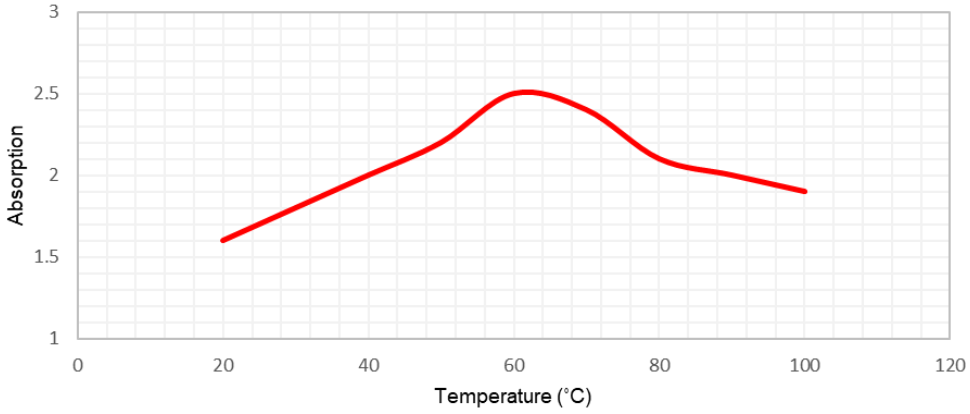

Fig. 7. Absorption of silver nanoparticles at different temperatures

intervals. The time required to reach the maximum absorption was determined as the optimal time. Fig. 6 illustrates that the optimal time for this green synthesis is 60 minutes.

5.5 Temperature optimization

In this step, solutions were prepared under the optimal conditions mentioned above. The mixture of extract and silver nitrate solutions was subjected to temperatures of 20, 30, 40, 50, 60, 70, 80, 90, and 100 degrees Celsius. The spectra of the mixtures were recorded using a UV/Vis spectrometer after the specified time intervals, as shown in Fig. 7. The highest absorption rate was observed at 60°C, which was determined as the optimal temperature.

Light interacts with sample molecules, resulting in the absorption of certain wavelengths of light while others pass through unchanged. The spectrophotometer presents the measurement results as a graph on the screen, with the vertical axis representing absorption (transition) and the horizontal axis representing wavelength. Each substance exhibits a unique absorption pattern in the UV-VIS spectrum, allowing for quantitative analysis of the material based on this spectrum.

Transmittance refers to the percentage of light that passes through a material. The amount of light transmitted

Table 2 Comparison of the synthesis of green silver nanoparticles using the extract of Lagoecia cuminoides L obtained with other silver nanoparticles

Plant name	Size (nm)	Morphology	Applications	Reference
Acacia nilotica (leaf)	20–50 (SEM	Spherical, uniform distribution	Antibacterial activity	(Ravikumar and Angelo 2015)
Aloe vera	5–50 (FE-SEM)	Octahedron	Antibacterial (Staphylococcu s aureus, Bacillus cereus, E. coli, Klebsiella pneumoniae, Micrococcus luteus) activity	(Logaranjan *et al*. 2016)
Piper betle (leaves)	156.4 (DLS)	Spherical	Antiquorum sensing and anti-biofilm activity against S. marcescens and P. mirabilis	(Srinivasan *et al*. 2018)
Curcuma longa (leaf)	15–40 (HR-TEM)	Spherical	The coating on the cotton fabric for antimicrobial and wound-healing activity	(Maghimaa and Alharbi 2020)
Origanum majorana	26.63 nm (TEM)	spherical	Potential Bioactivity against Multidrug Resistant Bacterial Strains	(Yassin *et al*. 2022)
This work	28 nm (TEM)	spherical	Antibacterial properties and a coating to prevent biological corrosion of underground pipes	

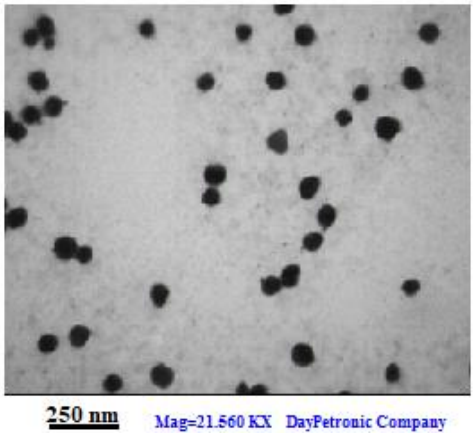

Fig. 8 TEM image of silver nanoparticles

through the material can be determined using the following equation: T (%) = I/I0 x 100 (where I0 represents the initial light intensity and I represents the transmitted light intensity). Typically, the transmittance value is expressed as a percentage. Absorption and transmission are closely related, and the amount of light absorbed is defined by the following relationship:

$$A = -\log T \quad (1)$$

The absorption (transmission) ratio is obtained by comparing the intensities of the transmitted and incident light. Consequently, physical units are canceled out in both the numerator and denominator of the fraction. This means that absorption and transmission rates are expressed without any physical units.

5.6 Comparison of synthesized silver nanoparticles with previously reported nanoparticles

Table 2 compares the properties of nanoparticles synthesized in this method with other previously synthesized silver nanoparticles. According to the comparison, the silver nanoparticle synthesized in this present method has a nanometer particle size and a spherical shape, similar to other methods. It exhibits microbiological anti-corrosion properties in deep soil that are superior to other nanoparticles. This makes it a promising candidate for applications in the oil and petrochemical industry.

5.7 Transmission electron microscope (TEM)

The transmission electron microscopic images related to the morphology of silver nanoparticles synthesized with Lagoecia cuminoides L in optimal conditions indicate the formation of nanoparticles with an approximate size of 28 nm. As shown in Fig. 8, the nanoparticles exhibit a spherical shape on the substrate.

5.8 Infrared spectrum (IR)

Different bonds and functional groups exhibit distinct absorption or transmission wave numbers. Therefore, it is necessary to examine the spectrum of the target substance to identify the presence or absence of specific functional groups and bonds. Reliable sources containing tables that report the vibration positions of different bonds in terms of wavelength or wave number can be utilized to identify various groups. In the case of organic substances, a list of potential groups and structures should be compiled, followed by a comparison of the spectrum with validated data from reliable sources. Additionally, reputable articles in databases can serve as valuable resources for analyzing FTIR spectra.

Fig. 9 illustrates the IR spectrum of green silver nanoparticles synthesized using Lagoecia cuminoides L plant extract. The resemblance between the IR spectrum of the extract and the nanoparticles indicates that the extract compounds form a layer around the nanoparticles, enhancing their stability. The presence of phenolic and alcoholic compounds is evident from the peaks observed at 3438 cm^{-1} and 3521 cm^{-1}, respectively. Furthermore, other peaks suggest the existence of carboxylic acid groups,

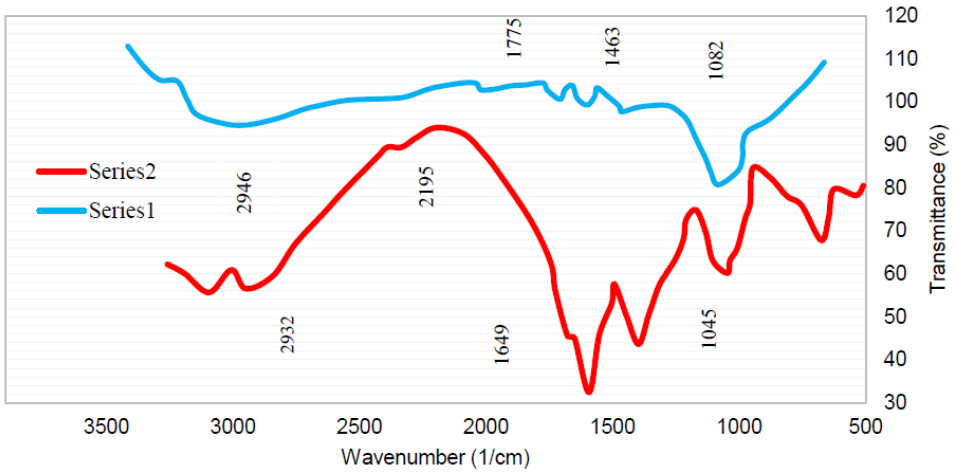

Fig. 9 Spectrum IR of silver nanoparticles (Series 1) and Lagoecia cuminoides L (Series 2) extract

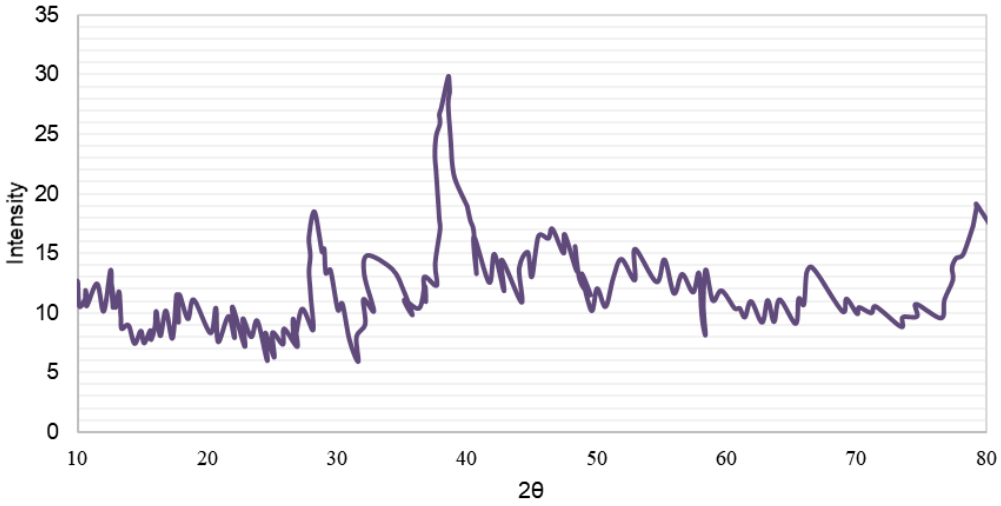

Fig. 10 X-ray diffraction pattern of silver nanoparticles

amides, and amines. The peak corresponding to the amino group provides evidence of protein presence in the nanoparticle structure. Plant proteins play a role in reducing silver ions, enveloping the nanoparticles, and preventing nanoparticle aggregation.

5.9 X-ray diffraction (XRD) analysis

The peaks observed in the X-ray diffraction pattern demonstrate an appropriate intensity, suggesting the formation of silver crystals (Fig. 10). The average particle size, estimated using Scherer's relation, is approximately 30 nanometers, consistent with the scanning electron microscope (SEM) results. Additionally, X-ray diffraction was employed as another test to confirm the production of nanoparticles, providing overall information about the chemical composition.

$$D = 0.9\lambda / \beta \cos \theta \quad (2)$$

In this context, 'λ' represents the wavelength of the X-ray, 'Θ' denotes the angle of the incident beam, 'β' refers to the peak width at half maximum intensity, and 'D' represents the approximate size of the particles.

5.10 Antibacterial effects of synthesized nanoparticles

The results indicate that the highest growth inhibition zone corresponds to a concentration of 100 micrograms per milliliter of synthesized silver nanoparticles. Conversely, the lowest growth inhibition zone is observed at a concentration of 25 micrograms per milliliter. These findings are presented in Fig. 11. Fig. 11.A1 and A2 display the culture medium of Staphylococcus aureus and Desulfococcus bacteria, respectively, in the absence of silver nanoparticles. On the other hand, Fig. 11.B1 and B2 depict the culture medium of Staphylococcus aureus and Desulfococcus bacteria, respectively, in the presence of silver nanoparticles.

The minimum inhibitory concentration (MIC) of the investigated nanoparticles for Staphylococcus aureus and Desulfococcus bacteria is determined as 0.92 µg/ml and 2.3 µg/ml, respectively. Furthermore, the minimum bactericidal concentration (MBC) of the biosynthesized silver nanoparticles against Staphylococcus aureus and Desulfococcus bacteria is determined as 2.37 µg/ml and 5.61 µg/ml, respectively. The MIC and MBC values obtained through the tube dilution method reveal that the minimum inhibitory

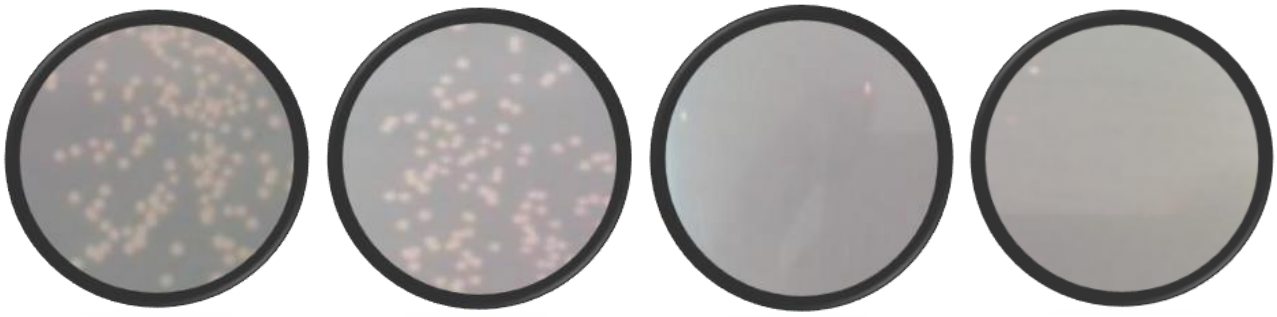

A1 A2 B1 B2

Fig. 11 Staphylococcus aureus and Desulfococcus bacteria culture medium without silver nanoparticles (A_1, A_2) and culture medium containing nanoparticles (B_1, B_2)

concentration of the nanoparticles against Staphylococcus aureus and Desulfococcus bacteria is 1.16 μg/ml and 2.32 μg/ml, respectively. The minimum bactericidal concentration of these nanoparticles against Staphylococcus aureus and Desulfococcus bacteria is determined as 2.46 μg/ml and 9.4 μg/ml, respectively. Thus, these nanoparticles exhibit potential for combating anaerobic bacteria responsible for the biological corrosion of steel pipes in the soil, thereby prolonging the lifespan of these pipes.

6. Discussion

In parallel with the rapid development of human life, it is imperative to control the harmful effects of microorganisms. The uncontrolled and rapid growth of microorganisms can lead to severe issues. The advancements in nanotechnology over the past decade have created excellent opportunities to explore the antibacterial properties of metal nanoparticles. The desired objective is to achieve antimicrobial modifications that inhibit bacterial growth. Nanomaterials incorporating metal ions exhibit significant antibacterial activity against bacteria, fungi, and viruses. Moreover, the antimicrobial characteristics of nanoparticles make them suitable for use in coatings applied to various implants, artificial teeth, artificial heart valves, and other medical devices. Steel pipes buried in the soil can be indirectly affected by heaving or swelling caused by microbial activity in the soil, leading to biological corrosion.

Microbial corrosion primarily occurs due to the presence of microorganisms that form biofilms on surfaces. Biofilms attach to the metal surface through weak intermolecular forces and are anchored by a secreted matrix. This matrix facilitates bacterial adhesion and acts as a substrate for additional bacteria, maximizing surface occupation. Once established, the biofilm can consist of millions of cells organized in multiple layers. Consequently, the metal surface becomes completely encapsulated by the biofilm layer.

In most cases, attempting to remove these layers using antibiotics and chemical agents proves futile due to the impermeable nature of the biofilm structure. Microbial degradation commonly results from specific bacterial genes that rely on nutrients present in water and soil. Sulfate-reducing bacteria (SRB) are the primary culprits responsible for biological corrosion, as they produce sulfuric acid. Thiooxidant bacteria often cause significant pipe damage in water and sewage systems. Anaerobic bacterial layers can exist within corrosion deposits. Applying a protective coating that separates the susceptible substrate from the electrolyte provides effective corrosion protection. Based on the outcomes of this study, the implementation of a green coating comprising silver nanoparticles can effectively prevent biological corrosion in pipes buried in the soil. The notable advantages of this method include biocompatibility, cost-effectiveness, avoidance of toxic and wasteful solvents, and the antimicrobial activity, making it suitable for large-scale commercial utilization.

7. Conclusions

The utilization of biological or green synthesis for nanoparticle production has garnered significant attention from researchers in the field of nanotechnology due to its health and environmentally friendly nature. In this study, silver was employed as both a reducing agent and stabilizer. We conducted an evaluation of the optimal conditions for the green synthesis of silver nanoparticles, aiming to avoid the use of toxic and hazardous substances. Reactive oxygen species, including superoxide anion radicals, were generated by silver ions, leading to increased intensity and induction of oxidative stress at the cellular, molecular, organ, and whole-cell levels. The presence of secondary metabolites such as phenols and flavonoids in plants conferred antimicrobial and antioxidant activities, effectively protecting cells against oxidative damage.

This research focused on investigating the green synthesis method utilizing the aqueous extract of Lagoecia cuminoides L for the production of silver nanoparticles and examining the antibacterial properties of the synthesized nanoparticles. The results demonstrated that the antibacterial activity of the synthesized silver nanoparticles was enhanced with increasing nanoparticle concentration. Therefore, this characteristic renders them suitable as a coating to prevent biological corrosion in underground pipes.

References

Alimoradlu, K. and Zamani, A. (2022), "Hydrophobicity in nanocatalysis", *Adv. Nano Res.*, **12**(1), 49-63. http://doi.org/10.12989/ANR.2022.12.1.049.

Alsultan Abdulmajeed, S. (2021), "Assessment of microstructure and surface effects on vibrational characteristics of public transportation", *Adv. Nano Res.*, **11**(1), 101-113. http://doi.org/10.12989/ANR.2021.11.1.101.

Azimi, M., Mirjavadi, S.S., Shafiei, N. and Hamouda, A.M.S. (2016), "Thermo-mechanical vibration of rotating axially functionally graded nonlocal Timoshenko beam", *Appl. Phys. A*, **123**(1), 104. https://doi.org/10.1007/s00339-016-0712-5.

Baalousha, M. (2009), "Aggregation and disaggregation of iron oxide nanoparticles: Influence of particle concentration, pH and natural organic matter", *Sci. Total Environ.*, **407**(6), 2093-2101. https://doi.org/10.1016/j.scitotenv.2008.11.022.

Bahmanzadegan, A., Rowshan, V., Zareiyan, F. and Hatami, A. (2019a), "Lagoecia cuminoides L., its antioxidant activity and polyphenolic constituents from Iran", *Nat Prod Res.*, **33**(16), 2376-2378.

Bahmanzadegan, A., Rowshan, V., Zareiyan, F. and Hatami, A. (2019b), "Lagoecia cuminoides L., its antioxidant activity and polyphenolic constituents from Iran", *Nat Prod Res.*, **33**(16), 2376-2378. https://doi.org/10.1080/14786419.2018.1440232.

Behdinan, K. and Moradi-Dastjerdi, R. (2022), "Thermal buckling resistance of a lightweight lead-free piezoelectric nanocomposite sandwich plate", *Adv. Nano Res.*, **12**(6), 593-603. http://doi.org/10.12989/ANR.2022.12.6.593.

Beyene, H.D., Werkneh, A.A., Bezabh, H.K. and Ambaye, T.G. (2017), "Synthesis paradigm and applications of silver nanoparticles (AgNPs), a review", *Sust. Mater. Technol.*, **13**, 18-23. https://doi.org/10.1016/j.susmat.2017.08.001.

Boulmedais, F., Frisch, B., Etienne, O., Lavalle, P., Picart, C., Ogier, J., Voegel, J.C., Schaaf, P. and Egles, C. (2004), "Polyelectrolyte multilayer films with pegylated polypeptides as a new type of anti-microbial protection for biomaterials", *Biomaterials*, **25**(11), 2003-2011. https://doi.org/10.1016/j.biomaterials.2003.08.039.

Cheng, F., Niu, B., Xu, N., Zhao, X. and Ahmad, A.M. (2023), "Fault detection and performance recovery design with deferred actuator replacement via a low-computation method", *IEEE T Auto Sci. Eng.*, 1-11. https://doi.org/10.1109/TASE.2023.3300723.

Cuong Bui, H. (2022), "Buckling analysis of thin-walled circular hollow section members with and without longitudinal stiffeners", *Struct. Eng. Mech.*, **81**(2), 231-242. https://doi.org/10.12989/SEM.2022.81.2.231.

Dai, W., Zand, Y., Sadighi, A.A., Selmi, A., Roco-Videla, A., Wakil, K. and Issakhov, A. (2021), "The economic and management use of rhododendron petals in potas-sium-ion nano batteries anode via efficient computer simulation", *Adv. Nano Res.*, **10**(6), 517-529. http://doi.org/10.12989/ANR.2021.10.6.517.

Ding, H.X. and She, G.L. (2021), "A higher-order beam model for the snap-buckling analysis of FG pipes conveying fluid", *Struct. Eng. Mech.*, **80**(1), 63-72. https://doi.org/10.12989/SEM.2021.80.1.063.

Dingreville, R., Qu, J. and Mohammed, C. (2005), "Surface free energy and its effect on the elastic behavior of nano-sized particles, wires and films", *J. Mech. Phys. Solids*, **53**(8), 1827-1854. https://doi.org/10.1016/j.jmps.2005.02.012.

Ebrahimi, F., Shafiei, N., Kazemi, M. and Mousavi Abdollahi, S.M. (2017), "Thermo-mechanical vibration analysis of rotating nonlocal nanoplates applying generalized differential quadrature method", *Mech. Adv. Mater. Struct.*, **24**(15), 1257-1273. https://doi.org/10.1080/15376494.2016.1227499.

Ehyaei, J., Akbarshahi, A. and Shafiei, N. (2017), "Influence of porosity and axial preload on vibration behavior of rotating FG nanobeam", *Adv. Nano Res.*, **5**(2), 141. https://doi.org/10.12989/anr.2017.5.2.141.

Farnsworth, N.R. and Soejarto, D.D. (1991), "Global importance of medicinal plants", *Conserv. Med. Plants*, **26**, 25-51.

Fu, Z.H., Yang, B.J., Shan, M.L., Li, T., Zhu, Z.Y., Ma, C.P., Zhang, X., Gou, G.Q., Wang, Z.R. and Gao, W. (2020), "Hydrogen embrittlement behavior of SUS301L-MT stainless steel laser-arc hybrid welded joint localized zones", *Corros. Sci.*, **164**, 108337. https://doi.org/10.1016/j.corsci.2019.108337.

Ghadiri, M., Hosseini, S.H.S. and Shafiei, N. (2016a), "A power series for vibration of a rotating nanobeam with considering thermal effect", *Mech. Adv. Mater. Struct.*, **23**(12), 1414-1420. https://doi.org/10.1080/15376494.2015.1091527.

Ghadiri, M., Shafiei, N. and Alavi, H. (2017a), "Thermo-mechanical vibration of orthotropic cantilever and propped cantilever nanoplate using generalized differential quadrature method", *Mech. Adv. Mater. Struct.*, **24**(8), 636-646. https://doi.org/10.1080/15376494.2016.1196770.

Ghadiri, M., Shafiei, N. and Alireza Mousavi, S. (2016b), "Vibration analysis of a rotating functionally graded tapered microbeam based on the modified couple stress theory by DQEM", *Appl. Phys. A*, **122**(9), 837. https://doi.org/10.1007/s00339-016-0364-5.

Ghadiri, M., Shafiei, N. and Babaei, R. (2017b), "Vibration of a rotary FG plate with consideration of thermal and Coriolis effects", *Steel Compos. Struct.*, **25**(2), 197-207. https://doi.org/10.12989/scs.2017.25.2.197.

Ghadiri, M., Shafiei, N. and Hossein Alavi, S. (2017c), "Vibration analysis of a rotating nanoplate using nonlocal elasticity theory", *J. Solid Mech.*, **9**(2), 319-337.

Ghadiri, M., Shafiei, N., Salekdeh, S.H., Mottaghi, P. and Mirzaie, T. (2016c), "Investigation of the dental implant geometry effect on stress distribution at dental implant–bone interface", *J. Brazil. Soc. Mech. Sci. Eng.*, **38**(2), 335-343. https://doi.org/10.1007/s40430-015-0472-8.

Guo, S., Zhao, X., Wang, H. and Xu, N. (2023), "Distributed consensus of heterogeneous switched nonlinear multiagent systems with input quantization and DoS attacks", *Appl. Math. Comput.*, **456**, 128127. https://doi.org/10.1016/j.amc.2023.128127.

He, H., Shuang, E., Ai, L., Wang, X., Yao, J., He, C. and Cheng, B. (2023), "Exploiting machine learning for controlled synthesis of carbon dots-based corrosion inhibitors", *J. Clean. Prod.*, **419**, 138210. https://doi.org/10.1016/j.jclepro.2023.138210.

Huang, S., Zong, G., Wang, H., Zhao, X. and Alharbi, K.H. (2023), "Command filter-based adaptive fuzzy self-triggered control for MIMO nonlinear systems with time-varying full-state constraints", *Int. J. Fuzzy Syst.*, 1-18. https://doi.org/10.1007/s40815-023-01560-8.

Iverson, W.P. (1987), *Microbial Corrosion of Metals*, Academic Press.

Kalajahi, S.T., Mofradnia, S.R., Yazdian, F., Rasekh, B., Neshati, J., Taghavi, L., Pourmadadi, M. and Haghirosadat, B.F. (2022), "Inhibition performances of graphene oxide/silver nanostructure for the microbial corrosion: molecular dynamic simulation study", *Environ. Sci. Pollut. Res.*, **29**(33), 49884-49897. https://doi.org/10.1007/s11356-022-19247-2.

Kashif, M., Sang, Y., Mo, S., Rehman, S.u., Khan, S., Khan, M.R., He, S. and Jiang, C. (2023), "Deciphering the biodesulfurization pathway employing marine mangrove Bacillus aryabhattai strain NM1-A2 according to whole genome sequencing and transcriptome analyses", *Genomics*, **115**(3), 110635. https://doi.org/10.1016/j.ygeno.2023.110635.

Kuang, F., Wang, J., Yan, L. and Zhang, D. (2007), "Effects of sulfate-reducing bacteria on the corrosion behavior of carbon

steel", *Electrochimica Acta*, **52**(20), 6084-6088. https://doi.org/10.1016/j.electacta.2007.03.041.

Li, H., Si, S., Yang, K., Mao, Z., Sun, Y., Cao, X., Yu, H., Zhang, J., Ding, C., Liang, H. and Wu, L. (2023), "Hexafluoro-isopropanol based silk fibroin coatings on AZ31 biometals with enhanced adhesion, corrosion resistance and biocompatibility", *Prog. Organ. Coat.*, **184**, 107881. https://doi.org/10.1016/j.porgcoat.2023.107881.

Liu, C., Cui, J., Zhang, Z., Liu, H., Huang, X. and Zhang, C. (2021), "The role of TBM asymmetric tail-grouting on surface settlement in coarse-grained soils of urban area: Field tests and FEA modelling", *Tunnell. Undergr. Space Technol.*, **111**, 103857. https://doi.org/10.1016/j.tust.2021.103857.

Logaranjan, K., Raiza, A.J., Gopinath, S.C.B., Chen, Y. and Pandian, K. (2016), "Shape- and size-controlled synthesis of silver nanoparticles using aloe vera plant extract and their antimicrobial activity", *Nanosc. Res. Lett.*, **11**(1), 520. https://doi.org/10.1186/s11671-016-1725-x.

Maghimaa, M. and Alharbi, S.A. (2020), "Green synthesis of silver nanoparticles from Curcuma longa L. and coating on the cotton fabrics for antimicrobial applications and wound healing activity", *J. Photochem. Photobiol. B*, **204**, 111806. https://doi.org/10.1016/j.jphotobiol.2020.111806.

Mousavi, S.M., Shafiei, N. and Dadvand, A. (2017), "Numerical simulation of subsonic turbulent flow over NACA0012 airfoil: evaluation of turbulence models", *Sigma J. Eng. Natural Sci.*, **35**(1), 133-155.

Nie, S., Mo, S., Gao, T., Yan, B., Shen, P., Kashif, M., Zhang, Z., Li, J. and Jiang, C. (2023), "Coupling effects of nitrate reduction and sulfur oxidation in a subtropical marine mangrove ecosystem with Spartina alterniflora invasion", *Sci. Total Environ.*, **862**, 160930. https://doi.org/10.1016/j.scitotenv.2022.160930.

Omidi, S., Oskooee, M.B. and Shafiei, N. (2013), "Finite element analysis of an ultra-fine grained Titanium dental implant covered by different thicknesses of hydroxyapatite layer", *Indian J. Dent.*, **4**(1), 1-4. https://doi.org/10.1016/j.ijd.2012.10.002.

Ran, C., Bai, X., Tan, Q., Luo, G., Cao, Y., Wu, L., Chen, F., Li, C., Luo, X., Liu, M. and Zhang, S. (2023), "Threat of soil formation rate to health of karst ecosystem", *Sci. Total Environ.*, **887**, 163911. https://doi.org/10.1016/j.scitotenv.2023.163911.

Ravikumar, S. and Angelo, R.U. (2015), "Green synthesis of silver nanoparticles using Acacia nilotica leaf extract and its anti-bacterial and anti oxidant activity", *Int. J. Pharmaceut. Chem. Sci.*, **4**(4), 433-444.

Shafiei, N., Ghadiri, M., Makvandi, H. and Hosseini, S.A. (2017), "Vibration analysis of Nano-Rotor's Blade applying Eringen nonlocal elasticity and generalized differential quadrature method", *Appl. Math. Modell.*, **43**, 191-206. https://doi.org/10.1016/j.apm.2016.10.061.

Shafiei, N., Hamisi, M. and Ghadiri, M. (2020), "Vibration analysis of rotary tapered axially functionally graded Timoshenko nanobeam in thermal environment", *J. Solid Mech.*, **12**(1), 16-32. https://doi.org/10.22034/jsm.2019.563759.1273.

Shafiei, N., Kazemi, M. and Ghadiri, M. (2016), "Nonlinear vibration behavior of a rotating nanobeam under thermal stress using Eringen's nonlocal elasticity and DQM", *Appl. Phys. A*, **122**(8), 728. https://doi.org/10.1007/s00339-016-0245-y.

Shahabinejad, E., Shafiei, N. and Ghadiri, M. (2018), "Influence of temperature change on modal analysis of rotary functionally graded nano-beam in thermal environment", *J. Solid Mech.*, **10**(4), 779-803. https://jsm.arak.iau.ir/article_545719.html.

Shivanian, E., Ghadiri, M. and Shafiei, N. (2017), "Influence of size effect on flapwise vibration behavior of rotary microbeam and its analysis through spectral meshless radial point interpolation", *Appl. Phys. A*, **123**(5), 329. https://doi.org/10.1007/s00339-017-0955-9.

Shokri, A. and Sanavi Fard, M. (2022), "Corrosion in seawater desalination industry: A critical analysis of impacts and mitigation strategies", *Chemosphere*, **307**, 135640. https://doi.org/10.1016/j.chemosphere.2022.135640.

Soltani, M., Moradi Kashkooli, F., Alian Fini, M., Gharapetian, D., Nathwani, J. and Dusseault, M.B. (2022), "A review of nanotechnology fluid applications in geothermal energy systems", *Renew. Sust. Energy Rev.*, **167**, 112729. https://doi.org/10.1016/j.rser.2022.112729.

Soltanieh, G., Yam Michael, C.H., Zhang, J.-Z. and Ke, K. (2022), "Closed-form solution for the buckling behavior of the delaminated FRP plates with a rectangular hole using super-elastic SMA stitches", *Struct. Eng. Mech.*, **81**(1), 39-50. https://doi.org/10.12989/SEM.2022.81.1.039.

Srinivasan, R., Vigneshwari, L., Rajavel, T., Durgadevi, R., Kannappan, A., Balamurugan, K., Pandima Devi, K. and Veera Ravi, A. (2018), "Biogenic synthesis of silver nanoparticles using Piper betle aqueous extract and evaluation of its anti-quorum sensing and antibiofilm potential against uropathogens with cytotoxic effects: an in vitro and in vivo approach", *Environ. Sci. Pollut. Res.*, **25**(11), 10538-10554. https://doi.org/10.1007/s11356-017-1049-0.

Tang, F., Wang, H., Zhang, L., Xu, N. and Ahmad, A.M. (2023), "Adaptive optimized consensus control for a class of nonlinear multi-agent systems with asymmetric input saturation constraints and hybrid faults", *Commun. Nonlinear Sci. Numer. Simul.*, **126**, 107446. https://doi.org/10.1016/j.cnsns.2023.107446.

Tang, S. and Zheng, J. (2018), "Antibacterial activity of silver nanoparticles: Structural effects", *Adv. Healthcare Mater.*, **7**(13), 1701503. https://doi.org/10.1002/adhm.201701503.

Tang, S.L.Y., Smith, R.L. and Poliakoff, M. (2005), "Principles of green chemistry: PRODUCTIVELY", *Green Chem.*, **7**(11), 761-762. https://doi.org/10.1039/B513020B.

Thakur, P., Chahar, D. and Thakur, A. (2022), "Visible light assisted photocatalytic degradation of methylene blue dye using Ni doped Co-Zn nanoferrites", *Adv. Nano Res.*, **12**(4), 415-426. http://doi.org/10.12989/ANR.2022.12.4.415.

Tian, H., Cui, Z., Ma, H., Zhao, P., Yan, M., Wang, X. and Cui, H. (2022), "Corrosion evolution and stress corrosion cracking behavior of a low carbon bainite steel in the marine environments: Effect of the marine zones", *Corros. Sci.*, **206**, 110490. https://doi.org/10.1016/j.corsci.2022.110490.

Uhlig, H.H. and Revie, R.W. (1985), *Corrosion and corrosion control*, Office of Scientific and Technical Information, U.S.A.

Vijayakumar, M., Priya, K., Nancy, F.T., Noorlidah, A. and Ahmed, A.B.A. (2013), "Biosynthesis, characterisation and anti-bacterial effect of plant-mediated silver nanoparticles using Artemisia nilagirica", *Ind. Crops Prod.*, **41**, 235-240. https://doi.org/10.1016/j.indcrop.2012.04.017.

Wang, J., Du, M., Li, G. and Shi, P. (2022a), "Research progress on microbiological inhibition of corrosion: A review", *J. Clean. Prod.*, **373**, 133658. https://doi.org/10.1016/j.jclepro.2022.133658.

Wang, J., Wang, Y., Ren, W., Zhang, D., Ju, P. and Dou, K. (2022b), ""Nano Killers" Activation by permonosulfate enables efficient anaerobic microorganisms disinfection", *J. Hazard. Mater.*, **440**, 129742. https://doi.org/10.1016/j.jhazmat.2022.129742.

Wang, Y.Y., Lou, M., Wang, Y., Wu, W.G. and Yang, F. (2022c), "Stochastic failure analysis of reinforced thermoplastic pipes under axial loading and internal pressure", *China Ocean Eng.*, **36**(4), 614-628. https://doi.org/10.1007/s13344-022-0054-3.

Wu, J., Zheng, J., Sun, G. and Chang, X. (2022), "Experimental and numerical analyses on axial cyclic behavior of H-section aluminium alloy members", *Struct. Eng. Mech.*, **81**(1), 11-28.

https://doi.org/10.12989/SEM.2022.81.1.011.
Wu, W., Xu, N., Niu, B., Zhao, X. and Ahmad, A.M. (2023), "Low-computation adaptive saturated self-triggered tracking control of uncertain networked systems", *Electronics*, **12**(13), 2771. https://doi.org/10.3390/electronics12132771
Yang, J., Wang, Z.B., Qiao, Y.X. and Zheng, Y.G. (2022), "Synergistic effects of deposits and sulfate reducing bacteria on the corrosion of carbon steel", *Corros. Sci*., **199**, 110210. https://doi.org/10.1016/j.corsci.2022.110210.
Yang, Y., Dou, Y., Wang, B., Xue, Z., Wang, Y., An, S. and Chang, S.X. (2023), "Deciphering factors driving soil microbial life-history strategies in restored grasslands", *iMeta*, **2**(1), e66. https://doi.org/10.1002/imt2.66.
Yassin, M.T., Mostafa, A.A.F., Al-Askar, A.A. and Al-Otibi, F.O. (2022), "Facile green synthesis of silver nanoparticles using aqueous leaf extract of Origanum majorana with potential bioactivity against multidrug resistant bacterial strains", *Crystals*, **12**(5), 603. https://doi.org/10.3390/cryst12050603.
Yuan, J., Li, Y., Shan, Y., Tong, H. and Zhao, J. (2023), "Effect of magnesium ions on the mechanical properties of soil reinforced by microbially induced carbonate precipitation", *J. Mater. Civil Eng*., **35**(11), 04023413. https://doi.org/10.1061/JMCEE7.MTENG-150.
Zehra, S., Mobin, M. and Aslam, J. (2022), *1 - An Overview of the Corrosion Chemistry*, Elsevier.
Zhang, C., Khorshidi, H., Najafi, E. and Ghasemi, M. (2023), "Fresh, mechanical and microstructural properties of alkali-activated composites incorporating nanomaterials: A comprehensive review", *J. Clean. Prod*., **384**, 135390. https://doi.org/10.1016/j.jclepro.2022.135390.
Zhang, G., Zhao, Z., Yin, X.-A. and Zhu, Y. (2021), "Impacts of biochars on bacterial community shifts and biodegradation of antibiotics in an agricultural soil during short-term incubation", *Sci. Total Environ*., **771**, 144751. https://doi.org/10.1016/j.scitotenv.2020.144751.
Zhao, K., Chen, Y., Yu, F., Jian, W., Zheng, M. and Zeng, H. (2022), "A biodegradable magnesium alloy sample induced rat osteochondral defect repair through Wnt/&#x03B2,-catenin signaling pathway", *Adv. Nano Res*., **12**(3), 301-317. http://doi.org/10.12989/ANR.2022.12.3.301.
Zhao, Y., Niu, B., Zong, G., Zhao, X. and Alharbi, K.H. (2023), "Neural network-based adaptive optimal containment control for non-affine nonlinear multi-agent systems within an identifier-actor-critic framework", *J. Franklin Inst*., **360**(12), 8118-8143. https://doi.org/10.1016/j.jfranklin.2023.06.014.
Zhu, Y. and Wu, X. (2023), "Heterostructured materials", *Prog. Mater. Sci*., **131**, 101019. https://doi.org/10.1016/j.pmatsci.2022.101019.

CC